



Seismic response analysis of RC framed buildings on geo-reinforced soil

M. V. Sreya¹ · B. R. Jayalekshmi² · Katta Venkataramana²

Received: 9 April 2021 / Accepted: 10 July 2023 / Published online: 26 July 2023
© Springer Nature Switzerland AG 2023

Abstract

Geotechnical seismic isolation is a recently emerged isolation technique to prevent the damaging effects of the earthquake on the building structures and nonstructural components. The study analyzes the effectiveness of different materials such as epoxy polystyrene, polyethylene foam, coir mat, rubber mat, and coir composites as a soil isolation medium to reduce the seismic energy transferred, thereby reducing the dynamic response of buildings under earthquake loads. Finite element analysis was carried out to evaluate the soil–structure interaction (SSI) effect in low-rise reinforced concrete structures with raft foundations subjected to various earthquake motions. Two kinds of soil, namely soft and stiff soil, were considered based on their flexibility to study dynamic soil–structure interaction effects. Roof acceleration and base shear of the building and contact pressure distribution and settlement at raft foundation–soil interface were the parameters evaluated for the different soil properties. The linear elastic behavior was assumed for the integrated building–foundation–soil system. This system was exposed to ground motions corresponding to scaled El Centro (1940) earthquake and simulated seismic excitation, which corresponds to the elastic design spectrum for Zone III as per the Indian standard code (IS 1893 (Part 1): 2016). The results indicate that the soil isolation provided by the high stiff polyethylene foam and coir mat substantially reduced the earthquake energy transmission to the superstructure. It is also observed that the seismic response of the buildings and raft is dependent on the flexibility of underlying soil. Seismic responses increase as the soil flexibility increases. Compared to stiff soil, the reinforced materials are very efficient in reducing seismic responses in soft soil.

Keywords Finite element simulation · Raft foundation · Soil isolation-building system · Soil reinforcement · Soil–structure interaction

Introduction

Raft foundations are provided in the form of a mat resting on soil that extends over the footprint of the building, reducing the soil pressure to support the facilities by transferring the loads to the soil. The stability of the whole superstructure depends entirely on the interface between the soil and foundation, irrespective of the physical nature of the soil of the building. The soil isolation method strengthens the soil by incorporating vibration-isolating

materials (geotechnical isolation) or providing vibration isolators in the construction (structural isolation). Geotechnical isolation is further classified as soil isolation and foundation isolation. The studies derived from the numerical analysis have demonstrated promising results in using recycled rubber [1] as seismic isolation material in the soil. Recycled rubber was used as an isolation medium to retain backfills provided with granular rubber soil mixtures, as an underground layer, it is used to mitigate the phenomenon of liquefaction or even as an isolation layer for structures. The scrap tires are used in various civil engineering applications such as slope stabilization, vibration isolation, retaining structures, road construction, ground erosion control, etc. The combination of sand and tire shreds helps strengthen the soil, both under static and dynamic loads. Shear strength is a significant parameter in certain studies [2] at the soil–tire interface. It was depicted that the rubber-stabilized (reinforced with a rubber mat),

✉ M. V. Sreya
sreya56vellur@gmail.com

¹ Department of Civil Engineering, St. Joseph Engineering College, Vamanjoor, Mangalore 575028, India

² Department of Civil Engineering, National Institute of Technology Karnataka, Surathkal, Mangalore 575025, India

highly rigid substratum ballast could significantly reduce the settlement and degradation in the ballast.

Another soil reinforcement material used is geofoms. The rigid plastic foams (geofoms) used in the light-weight filling [3, 4] for soft-ground construction, slope stabilization, wall or retaining wall isolation. The use of EPS blocks has also been extended to include geotechnical applications such as subbase fill materials [5–9], piers and bridge approach [4, 10–12], slope stabilization [13–17], earth retaining structures [18]. Some researchers have investigated the feasibility of using polyethylene fibers or strips in soil [11, 18, 19]. Polyethylene foam is a synthetic, excellent material that absorbs vibration energy and protects the structure. Plastic fibers and sheets are the major focus to improve and stabilize sandy soils, as fiber products are cost-competitive with other materials such as plastics. Polyethylene foams do not cause leaching problems and are not affected by chemical and biological degradation [20, 21].

The geotechnical base isolation system has been defined earlier by some researchers and the authors [8, 22–24]. They proposed the use of mixtures for low-cost seismic isolation using geosynthetics materials. The concept of geotechnical isolation includes a sliding mechanism with a low frictional coefficient by providing seismic isolation materials to dissipate seismic energy before it enters the superstructures. From the numerical analysis carried out [25] to evaluate the efficacy of the seismic isolation system based on geosynthetic reinforcement below the foundation, it was reported that the absolute acceleration at the roof level was reduced up to 40%. Experimental studies based on the shake table test have been done [25] by providing geotextiles and geomembranes as a base isolation system at the plinth level of a brick masonry building. However, the increased cost of geosynthetics and the growing value of biodiversity led researchers to concentrate more on natural resources as an alternative to conventional products.

Many natural materials in our surroundings can be used effectively for seismic isolation purposes. Coir is a type of natural material in the form of fibers processed into mat forms. Natural fibers such as coir were used in soil to increase their strength and decrease liquefaction [26, 27]. The length of soil-reinforced coir fiber is a factor studied because the long fibers have improved the resistance to liquefaction by limiting the interstitial pressures. The inclusion of coir fibers increases the resistance to liquefaction in cohesive soils. Even though the durability of the coir material is a matter of concern, as reported in Maheshwari et al. [28], the durability can be improved by coating fibers with phenol and bitumen. Chemical treatment of reinforcement material is one method to enhance durability and mechanical properties. The coconut fiber has

been chemically treated with alkali and silane at different concentrations [29–32].

The previous studies on seismic soil isolation techniques realize that an analysis should be carried out using other forms of polyethylene, coir, and rubber materials. There are studies on the use of these materials, mainly in the form of fibers and strips. Since the length of fiber helps increase the isolation efficiency of the reinforcement materials, the current study proposes reinforcing materials in their mat form. The literature survey observed that the EPS materials are used to strengthen soil behind the retaining wall, slope stabilization, etc. The application of EPS foams supports the shallow foundation for the structures, and its suitability as vibration absorbers has to be examined yet. The possibility of using low to high dense and stiff material is of great importance to study its effectiveness to act as the isolation materials.

This paper proposes the application of epoxy polystyrene geofom, polyethylene foam, rubber mat, and coir mat as vibration isolation materials in the soil. The composite materials, coir–polyethylene foam, and coir–rubber mats are introduced in the soil to improve the service life of reinforced coir mat and enhance the isolation efficiency of strengthening material. This study also compares the efficacy of natural and synthetic materials in the form of mats within the soil as vibration absorbers by investigating the different seismic responses of the soil–structure system. The soil stiffness is considered while designing raft foundations to understand the load distribution in the raft foundation. Three-dimensional finite element models of integrated building–raft–soil systems were developed and analyzed with and without a mechanism of soil isolation, incorporating the flexibility of soil in the time domain.

Soil–structure interaction

The structural response to an earthquake is interconnected by three systems, such as structure, foundation, and soil. Studying the soil–structure interaction is essential when seismic forces significantly impact the base movement compared with the free activity in the soil. Two fundamental approaches, namely direct method and substructure, are used to solve the soil–structure interaction (SSI) problems [33]. The direct SSI method is employed to model and analyze the entire soil structure in a single phase. In this study, the SSI method was selected wherein the soil and structure are modeled together. Many recent studies [34] utilized this method for the SSI analysis of complex structures using powerful computing efficiency in most modern computers. In the substructure approach, the soil–structure system is divided into two substructures, the soil medium and the structures. This method is based on the principle of superposition. One

of the drawbacks of this method is that only linear systems can be analyzed. The main advantage of the direct method compared to the substructure method is that it can consider the nonlinear material behavior [35, 36].

Some studies have reported the detrimental effect of SSI in buildings [37–39]. But limited research has been done in three-dimensional SSI analysis of buildings, including foundation-isolated soil systems. The current study analyses the different materials-reinforced and unreinforced soil–structure interaction from their seismic responses under earthquake loading.

Description of the problem

Studies on soil reinforcement with different materials have been described in the literature [1, 7, 8, 11, 24, 32, 40, 41]. But the application of reinforcement materials for the soil isolation for shallow foundations are very few. Moreover, the application of reinforcement materials in their mat form for shallow foundations is not detailed in the literature. Studies [42] reveal that the isolation efficiency of reinforcement fibers increases with fiber length. Therefore, the concept of introducing the commonly available reinforcement materials in their mat form is addressed in this study. The current investigation consists of a response evaluation of multistory buildings with raft foundations resting on different soil types and subjected to earthquake loads. The three-dimensional finite element model of the integrated building–foundation–soil system was analyzed based on the direct SSI method in which analysis of structure and soil is carried out in a single step. The resulting contact pressure and settlement at the raft–soil interface and building seismic responses such as roof acceleration and base shear were assessed by incorporating the SSI effects corresponding to different soil flexibility. Also, the efficacy of other materials as soil-isolation in reducing structural response is investigated.

Idealization of structure

The model studied includes four-bay five-storey RC framed buildings supported by the raft foundation resting on different soil. The bay length of building frames was 4 m, and the storey height is 3 m. The cross sections of the beams and columns were taken as 300 mm × 300 mm and 500 mm × 500 mm, respectively. Floor and roof slabs were provided with a thickness of 150 mm. Based on structural specifications as per Indian standard codes for the design of reinforced concrete structures, IS 456:2000 and IS 13920:1993, dimensioning of slabs, beams, and reinforced concrete structures were determined. Raft size was taken as 18 m × 18 m with a thickness of 1 m. Apart from the dead

load due to the self-weight of the structural elements, the live load on floors was 3kN/m². The M25 grade concrete and Fe, 415-grade steel, was selected as the building and raft materials. The modulus of elasticity (E_c) for building and raft foundation, 25GPa, was calculated corresponding to M25 grade concrete using the equation,

$$E_c = 5000\sqrt{f_{ck}} \tag{1}$$

where f_{ck} is the characteristic compressive strength of concrete after 28 days, the Poisson’s ratio and unit weight of concrete were taken as 0.15 and 25kN/m³, respectively, for both building and raft foundation.

The configuration of the soil–structure system is depicted in Fig. 1a. Finite element simulation of transient response was carried out on these three-dimensional field-scale models with and without soil-isolation mechanism. The soil–structure system without isolation is represented as 'UR.'

Idealization of infinite soil

An elastic continuum finite element model was assumed to represent the soil for the analysis. Since soil is a semi-infinite medium, as per Wolf [33], the boundary should be placed at a distance away from the foundation laterally, where the static responses of the system die out. The boundaries of soil were placed about 4.5 times the raft width from each side of the foundation. The bedrock was assumed to be at a depth of 30 m for all models considered so that a finite

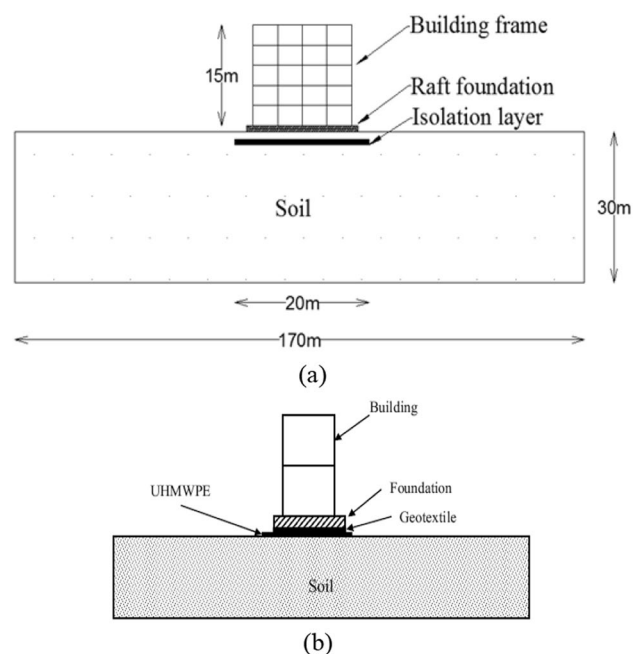


Fig. 1 The configuration of the isolated soil-building system

domain is considered for the analysis. The soil stratum size was 170 m \times 170 m with a depth of 30 m (Fig. 1). Nonreflecting boundaries were assigned at lateral boundaries to represent an infinite soil stratum. The Young's modulus and Poisson's ratio of the soil were adopted corresponding to soft soil (S_1) ($V_s < 150$ m/s) and stiff (S_2) soil ($150 < V_s < 300$) as per the standards of NEHRP guidelines for the seismic rehabilitation of buildings from FEMA 273 [FEMA 273-1997 and FEMA 356-2000]. The unit weight of the soil was taken corresponding to the flexibility of the soil. The details of the various soil properties used in the analysis are listed in Table 1.

Idealization of the isolation layer

Ground improvement with soil reinforcement is a standard method practiced. The addition of strengthening elements improves the engineering properties of soil. The reinforcing materials absorb the tensile load and the shear stresses within the soil structure, thereby preventing shear or excessive deformations. Suitable material must be chosen for the reinforcement so that shear stress, shear force, and lateral deformation of the material under the dynamic load should be minimum. The materials used for seismic isolation in the form of mats were coir mat (C), epoxy polystyrene (EPS), rubber mat (RU), polyethylene foam of low stiffness (PE_1), polyethylene foam of high stiffness (PE_2), composite of coir mat and rubber mat (C-RU), composite of coir mat and polyethylene of high stiffness (C- PE_2). The detailed properties

Table 1 Properties of soil

Soil type	Description of soil	Shear wave velocity, V_s (m/s)	Poisson's ratio	Unit weight (kN/m^3)
S_1	Soft soil	120	0.4	16
S_2	Stiff soil	270	0.35	18

Table 2 Properties of building components and isolation materials

Specification	Dimension	Young's Modulus of elasticity (MPa)	Poisson's ratio	Unit weight (γ_d), (kN/m^3)
RC Beam (B \times D \times L)	0.3 m \times 0.3 m \times 4 m	25×10^3	0.15	25
RC Column (B \times D \times L)	0.5 m \times 0.5 m \times 3 m	25×10^3	0.15	25
Raft foundation (B \times D \times L)	18 m \times 18 m \times 1 m	25×10^3	0.15	25
Rubber mat (B \times W)	20 m \times 20 m	100	0.49	15
Coir mat (B \times W)	20 m \times 20 m	4100	0.3	15
EPS geof foam (B \times W)	20 m \times 20 m	22	0.1	0.22
Polyethylene foam ₁ (B \times W)	20 m \times 20 m	150	0.2	4
Polyethylene foam ₂ (B \times W)	20 m \times 20 m	900	0.2	4

of various isolation materials used in the analysis are listed in Table 2.

The depth of placement of reinforcement plays a vital role in reducing the seismic responses under dynamic loads. An optimum depth helps to intercept the shear zone as much as possible and induces optimum lateral retention of the deformed zone under the raft foundation. The reinforcement mats were placed at an optimum depth of 1 m for EPS geof foam, polyethylene foam, and rubber mat. For natural materials such as coir mat, coir-rubber, and coir-polyethylene composite, the depth of placement was taken as 2 m to be secured against external sources of degradation and weathering. All the reinforcement mats provided were 2 m thickness having a planar dimension of 20 m \times 20 m, which covers the bottom area of the raft foundation with 1 m extensions in all four directions. Coir composites were modeled with each layer of composite materials having a thickness of 0.5 m provided at top and bottom sandwiched with 1 m of coir mat in the middle to get an adequate total thickness of 2 m.

Finite element modeling of the building-raft-soil system

The integrated building-raft-soil system was analyzed by the finite element method using ANSYS software, assuming its linear elastic behavior. The building frame was modeled using a two-node linear beam element, i.e., BEAM188. The soil stratum was discretized with eight-node linear brick reduced integration element, i.e., SOLID 185. It is a first-order element with linear interpolation in each direction, and it is suitable for convergence in contact analysis. Soil medium was discretized with solid elements of size in the order of 0.5, 1, 2.5, 5, and 10 m along the lateral direction with fine mesh near the structure, which gradually increases to a coarser mesh away from the structure. Raft foundation was also discretized with eight-node linear brick reduced integration elements as that of soil. Raft volume was discretized with elements of size 1 m. As the reinforcement materials used for isolation undergo bending under load, it

was modeled with 3D finite strain 190, SOLSH190 element having very low bending stiffness. Soil isolation mats were meshed with 0.5 m size. Nonreflective boundaries on the lateral boundary surfaces of the soil media were assigned to represent the infinite soil medium. The lateral sides of the soil were modeled with viscous boundaries so that the non-reflecting effect under dynamic loading can be represented. COMBIN 14 elements were used for viscous boundary, and proper damping and stiffness values corresponding to the soil were assigned. The soil stratum base was set as fixed so that any motion and moments would be prevented. Three-dimensional finite element modeling of the whole building–raft–soil system was generated using the ANSYS software and is shown in Fig. 2. Altogether, 34,299 nodes and 29,409 elements, including 6400 solid shell reinforcement elements, were used for the model. CONTACT and TARGET elements were used to model the interface of soil and isolation materials. The interface between the underneath soil and isolation materials formulated with a coefficient of friction values. The coir mat coefficient [40, 43] and rubber mat were given as 0.5, and for EPS [44, 45] and polyethylene foam, it was given as 0.7.

Methodology

The time history analysis of the integrated soil–structure system was carried out with ground motion corresponding to the longitudinal component of the Imperial Valley earthquake at El-Centro (1940) with modified peak ground acceleration (PGA) of 0.3 g as well as simulated seismic excitation corresponding to Zone III as per IS 1893:2016 with PGA of 0.1 g. The input motions corresponding to modified El Centro ground motion and simulated ground motion corresponding to the Zone III design spectra of IS 1893 (2016) are designated as El Centro and IS input motion. The input

ground motions were chosen based on the availability of high-amplitude frequency content that matches the natural frequency of the soil–structure system. The resonance effect demonstrates the highest seismic response in the superstructure under the ground excitations. The FFT analysis shows that the peak value of Fourier amplitude occurs at a frequency range of 1.1–1.4 Hz for the El Centro and IS input motion. Table 3 lists the natural frequencies of the soil–structure systems considered for the analysis. The natural frequency of soil–structure systems considered for soft soil obtained from the modal analysis was almost the same, and it was increased for stiff soil. The total duration of the ground motion was taken as 30 s for the El-Centro earthquake and bracketed duration of 17.81 s for the IS input motion. The acceleration time history plot of input ground motions and corresponding FFT is shown in Fig. 3. These two ground motions were applied in the global X direction of the soil–structure model in ANSYS. Five-storey buildings, as described in Sect. 3.3, were considered for the transient analysis.

Table 3 Natural frequencies of the soil–structure system

Isolation mat	Natural frequency of soil–structure model (Hz)	
	Soft soil	Stiff soil
EPS	1.1212	1.3336
RU	1.1212	1.3529
PE ₁	1.1212	1.3533
PE ₂	1.1212	1.3621
C	1.1212	1.3656
C-RU	1.1212	1.3622
C-PE ₂	1.1212	1.3617
UR	1.1212	1.3590

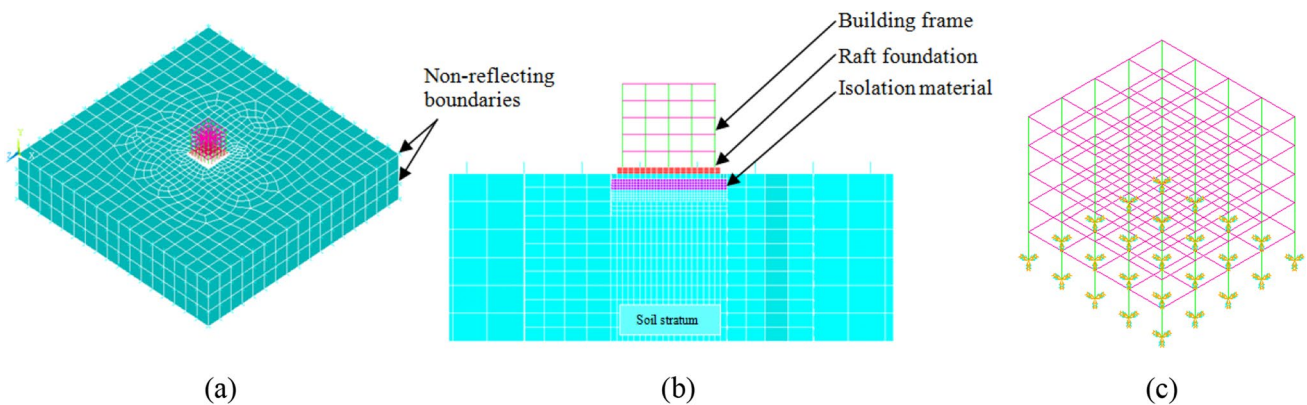


Fig. 2 Finite element model of the building–raft–soil system in ANSYS Software **a** Isometric view, **b** Cross-sectional view for the reinforced soil–structure model, **c** Fixed-base model

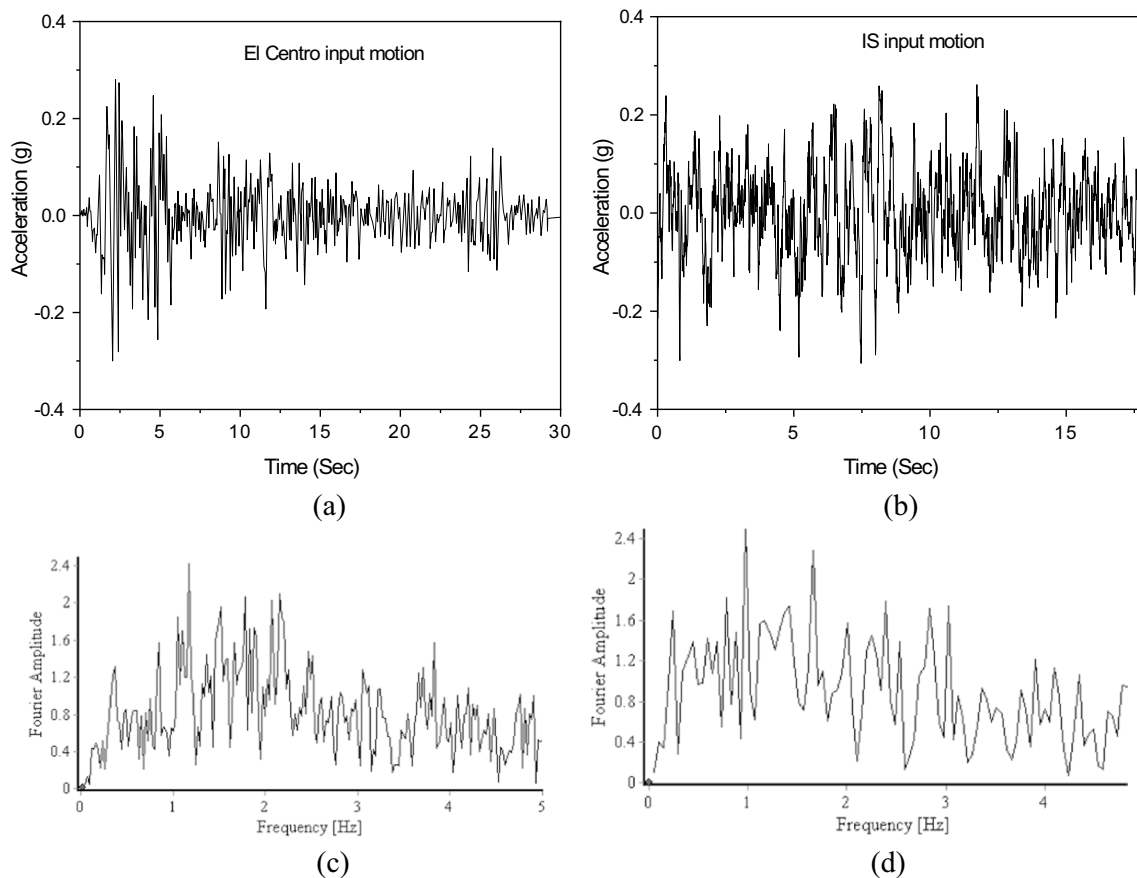


Fig. 3 a Acceleration time history of El Centro b acceleration time history of IS c FFT diagram-El Centro d FFT diagram-IS

The integrated building–soil system with and without soil isolation mechanism was studied by incorporating the soil reinforcement with different isolation materials. Case 1 and Case 2 are defined to group the isolation materials. The materials used in case 1 represent EPS, RU, PE₁, and PE₂ mats. The coir mat and its composites such as C, C-RU, and C-PE₂ mats are re-referred to as Case 2 materials. Both reinforced and unreinforced soil models were analyzed under seismic load for models resting on the two different types of soil. Comparative analysis of seismic responses of buildings founded in isolated and conventional soil stratum would provide isolation performance of the material. Contact pressure distribution at the soil–raft interface was studied for traditional and isolated cases of models. The slip deformation of the reinforcement and the soil was found to be a critical parameter from the dynamic response of the geosynthetic–soil interface during harmonic excitation [22].

A nondimensional factor, reduction factor (RFs) to express the reduction in the settlement below the raft under earthquake excitations is introduced as.

$$RFs = \frac{S_u}{S_r} \tag{2}$$

where

S_u : Settlement of the raft foundation on unreinforced soil model.

S_r : Settlement of the raft foundation on reinforced soil model.

Contact pressure reduction below the raft foundation also has been expressed in terms of reduction factor, i.e., (RFc) (Eq. 3).

$$RFc = \frac{C_{pu}}{C_{pr}} \tag{3}$$

where

C_{pu} : Contact pressure developed below the raft foundation on unreinforced soil.

C_{pr} : Contact pressure developed below the raft foundation on reinforced soil.

The isolation efficiency of reinforced mats has been defined as follows;

$$\text{Isolation efficiency of reinforced mats} = \frac{\text{Seismic response}(u) - \text{Seismic response}(r)}{\text{Seismic response}(u)} \tag{4}$$

where

Seismic response (u): Seismic response of the unreinforced soil–structure system.

Seismic response (r): Seismic response of the reinforced soil–structure system.

Thus, the higher the reduction factor, a higher the isolation effect and higher the isolation efficiency (Eq. 4) for the particular reinforcement mat in the soil stratum.

Seismic building responses such as roof acceleration and base shear were evaluated to study the isolation performance of reinforcement materials in the soil. Seismic base shear is the highest lateral force exerted during the seismic event on the building at its base. Here, the seismic base shear of the building resting on different isolation mat-reinforced soil stratum has been represented in terms of the total weight of the building as the base shear ratio (Eq. 5).

$$F' = \frac{F}{W} \tag{5}$$

F' : Base shear ratio of building.

F : Shear force at the base of the building.

W : Total weight of the building.

Validation

The finite element program 'ANSYS' is used to analyze the soil–structure system. The numerical model of soil–structure system carried out by Nanda et al. [25] in ABAQUS software is validated in this study by using ANSYS. The isolation scheme uses a high-strength nonwoven geotextile–geomembrane [ultrahigh molecular weight polyethylene (UHMWPE)] interface. Three-dimensional buildings G + 1, G + 2, and G + 3 one-bay moment-resisting RC frames are considered to estimate seismic response at the roof level with and without isolation mechanism (Fig. 1b). The Typar 3601 geotextile and 6.4 mm thick UHMWPE interfaces are simulated with a dynamic friction coefficient of 0.07. A

friction coefficient of 0.3 is also formulated for the interface between the underlying soil and the UHMWPE. The soil and raft foundation discretized with eight linear brick node reduced integration element, i.e., hourglass control (C3D8R). Two-node linear beam element in surface, i.e., B31, is used to model the buildings.

The results obtained from the numerical analysis of the model using ANSYS software are compared with the outcomes of Nanda et al. [25]. The validated model results are in good agreement with the numerical work reported, as shown in Table 4. Peak absolute acceleration values at the roof level for conventional G + 2 and G + 3 buildings from the ANSYS software results match obtained from the paper with a slight variation of 1.8 and 2.1%, respectively. But the absolute peak values for the isolated buildings were varied by 1 and 0.5%, respectively.

Results and discussion

The seismic responses of the soil–structure system analyzed and findings were compared to select the best isolation material.

Effect of soil flexibility

Soil–structure interaction effects on the seismic response of structures depend mainly on soil flexibility [46, 47]. Two types of soils, namely S_1 and S_2 representing soft and stiff soil, were considered to identify the effect of SSI. It is observed from the analysis that the natural frequency of the SSI system (Table 3) was lower than the natural frequency of the fixed-base structure (1.96 Hz), and about 43% reduction in natural frequency was noticed when the underlying soil was soft.

For fixed-base models and buildings, which rest on the soft and stiff soil stratum, the effect of SSI on seismic responses in terms of roof acceleration was analyzed. Figure 4 indicates that seismic responses increase as soil flexibility increases. The roof acceleration of the building is increased by about 70 and 33%, respectively, in soft and stiff conventional soil base supported system, compared to the fixed-base system subjected to El Centro input motion. Therefore, SSI has a significant role in the seismic behavior

Table 4 Comparison between absolute roof response analysis results from ANSYS and ABAQUS software

Building	Earthquake	Peak absolute acceleration at roof level (g) ABAQUS		Peak absolute acceleration at roof level (g) ANSYS	
		Conventional building	Isolated building	Conventional building	Isolated building
G + 2	El Centro	2.224	1.457	2.182	1.756
G + 3	El Centro	2.074	1.215	2.029	1.221

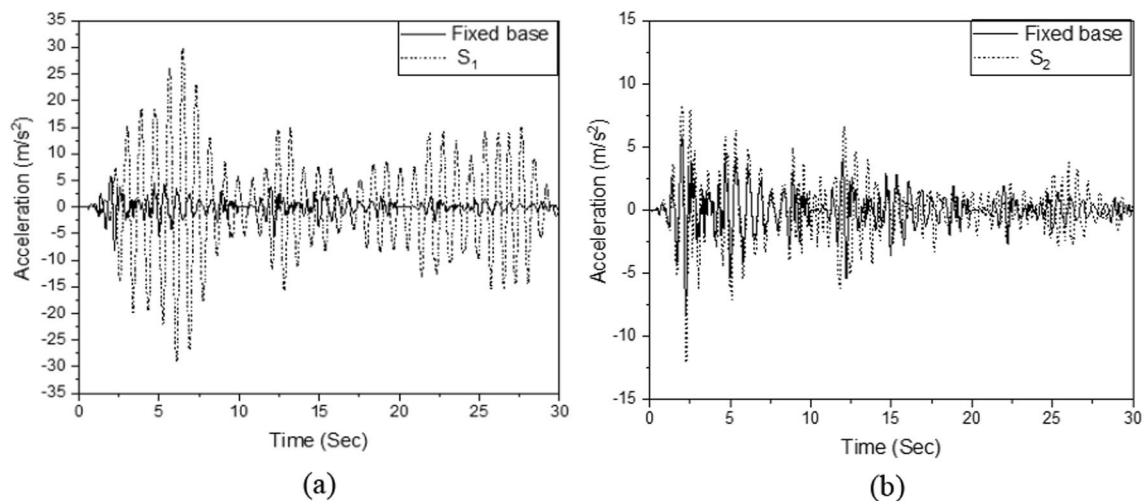


Fig. 4 Time history of absolute roof acceleration in building with a fixed base and building on **a** soft (S_1) and **b** stiff soil (S_2)

of structures. Since the seismic responses shown by building resting on soft and stiff soil are higher than that on a fixed base, seismic soil isolation is addressed. The following section compares the seismic responses of different mats reinforced soil–structure systems.

Absolute roof acceleration of building

Roof acceleration response of the five-storey building was evaluated for the cases of unreinforced and reinforced soil base. The isolation capacity of case 1 and case 2 soil reinforcing materials were compared by incorporating the soil flexibility (Fig. 5). The percentage reduction in roof acceleration of buildings on various mats reinforced soil compared to unreinforced soil is evaluated. Figure 6 shows the time history of acceleration for soil–structure system reinforced with coir mat in soft and stiff soil excited under El Centro and IS input motions.

From the proposed study of soft soil strengthened with mats of case 1 material, such as EPS, RU, PE_1 , and PE_2 mats, respectively, subjected to El Centro input motion, a reduction of 2.6, 9.8, 15.1, and 23% in the roof acceleration is observed (Fig. 5a). The roof acceleration does not reduce with the EPS mat reinforced soil base. In comparison with low stiff polyethylene (PE_1), a high stiff polyethylene mat (PE_2) reinforced soil system shows about 1.6 times higher percentage reduction in roof acceleration (Fig. 5a).

In stiff soil, the reinforced mats do not show a noticeable reduction in roof acceleration than soft soil. EPS mat reinforcement in stiff soil exhibits improved performance, around 3% reduction, than any other isolation mats (Fig. 5b). In screening the high-frequency dynamic source besides turbo generators, turbines, etc., continuous EPS geof foam was more efficient. For comparatively more stiff

soil deposition, EPS geof foam works well [27]. In reducing roof acceleration of buildings resting on stiff soil, the efficacy of low stiff and high stiff polyethylene mat reinforcement does not vary significantly. The rubber mat does not contribute to the same at all (Fig. 5).

The soil–structure system, in which the soil is reinforced with mats of case 1 materials, excited under IS input motion, is analyzed. The reduction in building roof acceleration is achieved with all the reinforcement mats. The percentage reduction in roof acceleration obtained for building resting on the soft soil is in the range of 2–9% with reinforcement of all the isolation mats (Fig. 5c). Compared with low stiff polyethylene (PE_1), a high stiff polyethylene mat (PE_2) reinforced soil system shows about two times higher percentage reduction in roof acceleration. In stiff soil, the reduction of 5% in roof acceleration is observed with reinforcement of PE_1 and PE_2 mats only (Fig. 5d).

From the analysis of soft soil reinforced with mats of case 2 materials, it is observed that the roof acceleration is reduced by about two to eight times more than that observed from soft soil reinforced with the mats of case 1 material EPS, RU, and PE_1 . Combining two highly stiff materials resulted in a better composite mat, C- PE_2 , which significantly reduces the seismic response. The peak roof acceleration response of the building on coir mat and C- PE_2 mat strengthened soil is decreased by 19 and 22%, respectively, compared to the unreinforced soil (Fig. 5c). And this reduction is 18% with C-RU mat reinforcement. The coir mat reinforced soil stratum shows only 2.2% isolation efficiency to reduce roof acceleration in stiff soil.

Under the IS input motion, the roof acceleration response of the soil–structure system in which the soft soil is strengthened by mats of case 2 materials is analyzed. The percentage

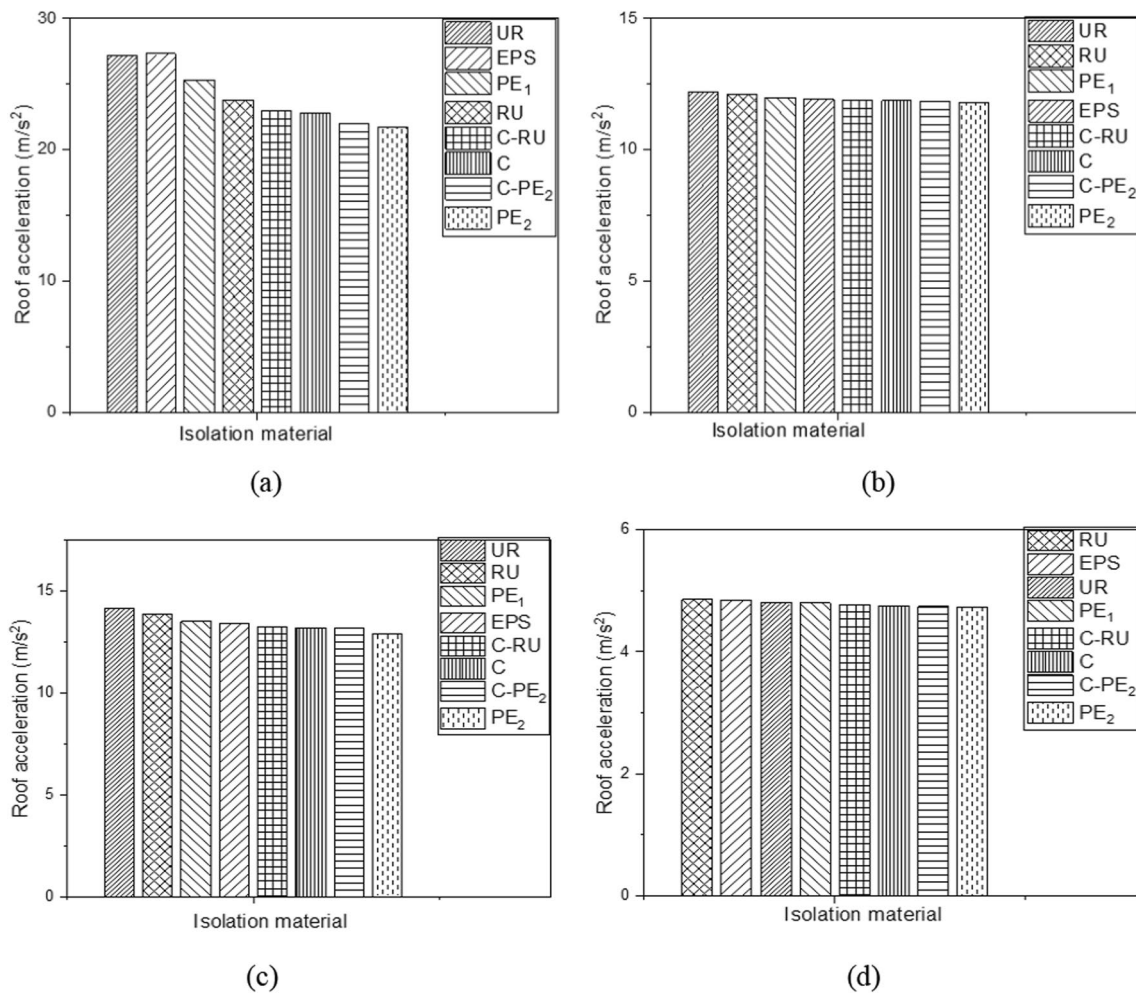


Fig. 5 Roof acceleration for soil reinforced with different isolation mats **a** El Centro-soft soil **b** El Centro-stiff soil **c** IS-soft soil **d** IS-stiff soil

reduction of 6.4, 6.8, and 6.9%, respectively, is observed in C-RU, C, and C-PE₂ mat enhanced soil base (Fig. 5c). In stiff soil, roof acceleration is reduced with the reinforcement of all the case 2 materials, but the reduction is not significant, i.e., less than 5% (Fig. 5d).

Absolute roof acceleration response of a five-storey building-isolated soil system excited under two different input motions, incorporating the soil flexibility is evaluated. The observed roof acceleration responses under input motions of El Centro are more advantageous than that with IS input motion, as El Centro motions have high peak acceleration amplitudes compared to IS input motion (peak ground acceleration of El Centro and IS input motion is 0.3 and 0.1 g, respectively). This roof acceleration response in buildings resting on stiff soil is lower than in soft soil as the stiff soil has lower amplification than soft soil. It is also observed that isolation materials work better in soft soil than in stiff soil to mitigate seismic response. A highly stiff polyethylene mat shows around 23–33% more isolation efficiency than the

coir mat in reducing the roof acceleration of the building (Fig. 5a–d).

It is not technically feasible to have highly stiff polyethylene material as a soil reinforcement material for a 2 m thickness; however, composite of coir mat and polyethylene is practically possible. With advantage for isolation purposes, the composite of coir mat and polyethylene foam may also act as a suitable drainage medium (Table 5).

High stiff polyethylene has been chosen to make a composite with a coir mat since the high stiff polyethylene mat shows around two times more isolation efficiency than low stiff polyethylene foam. The rubber mat gives better isolation efficiency and works as a good composite with the coir mat. It is a combination of low and high stiff synthetic and natural materials having the same density. Generally, isolation materials and pile foundations are practiced to mitigate the seismic response of multistorey buildings. For example, rubber mixed in the form of tire chips in the sand for 5 m thickness and piles to isolate seismic responses showed an isolation efficiency of around 40% for roof acceleration in

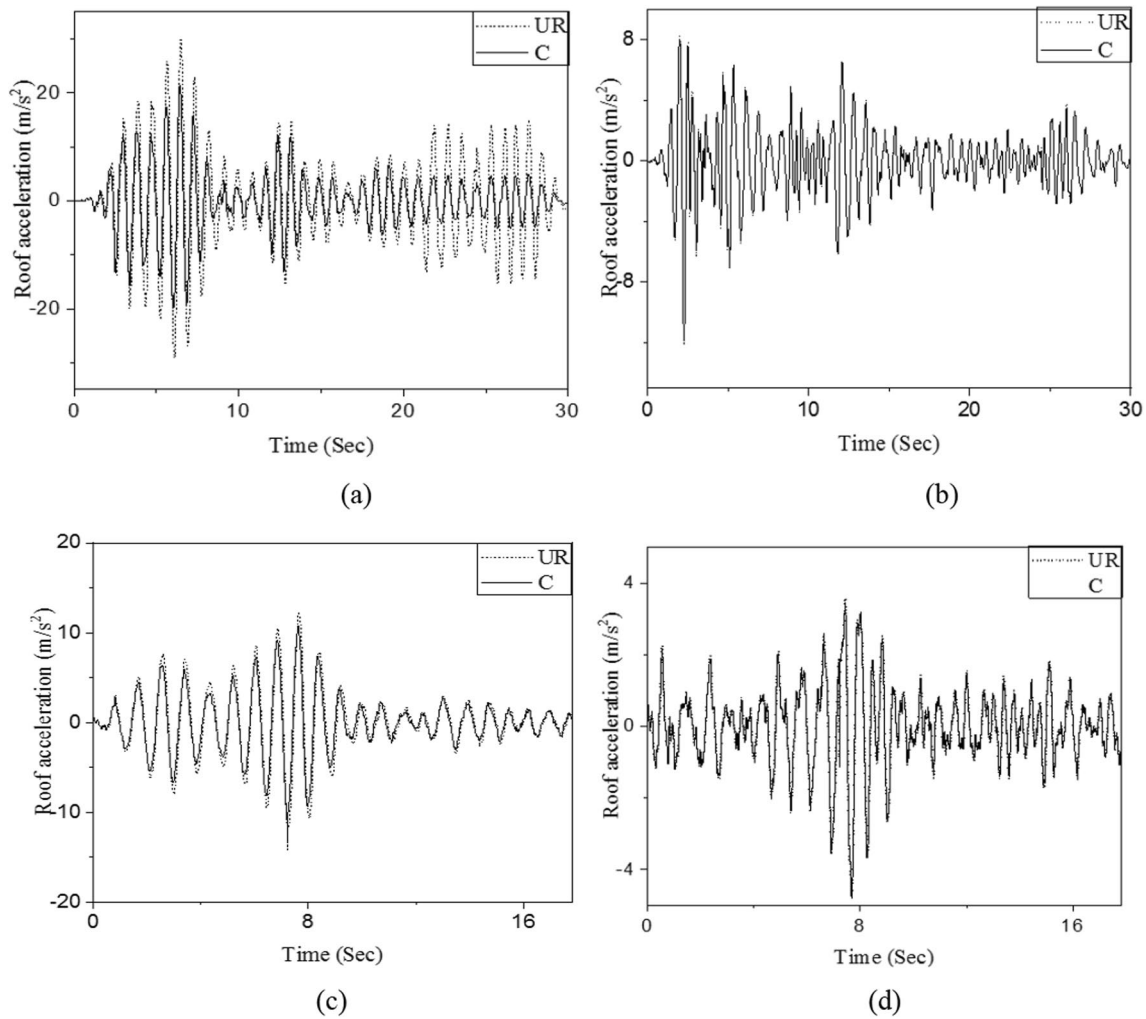


Fig. 6 Roof acceleration time history plot of the soil–structure system for unreinforced and reinforced cases of S_1 and S_2 type soil with coir mat under **a** El Centro-soft soil **b** El Centro-stiff soil **c** IS-soft soil **d** IS-stiff soil

five-storey buildings [36]. But in this proposed study, the reinforcement of isolation mats only with 2 m thickness reduces the roof acceleration response of the building significantly with a maximum reduction factor of 23% (Fig. 5).

Seismic base shear of building

The base shear ratio variation (base shear divided by the weight of building) obtained by considering the fixed base and incorporating the three-dimensional soil–structure interaction (SSI) effect is examined. The isolated soil–structure system analyzed and compared the isolation efficiency of reinforced mats to reduce this base shear. The base shear ratio is noted and represented in terms of the total weight of the superstructure (Fig. 7). It is observed here that the seismic base shear is more than the fixed-base condition when the SSI effects are taken into consideration (Table 6) [48]. With an increase in soil flexibility, the seismic base shear is increased. Isolation mats show a noticeable reduction in soft soil than in stiff soil. Same results were observed from the previous results also. When the soil is soft to medium, the response is significantly higher than that of the bridge with a fixed tower

Table 5 Fourier amplitude and specific energy density corresponding to the natural frequency of the soil–structure system with isolation

Earthquake	Fourier amplitude		Specific energy density (m^2/s)
	Soft soil (1.12 Hz)	Stiff soil(1.35 Hz)	
El Centro	0.974	1.443	0.199
IS	0.471	0.543	0.052

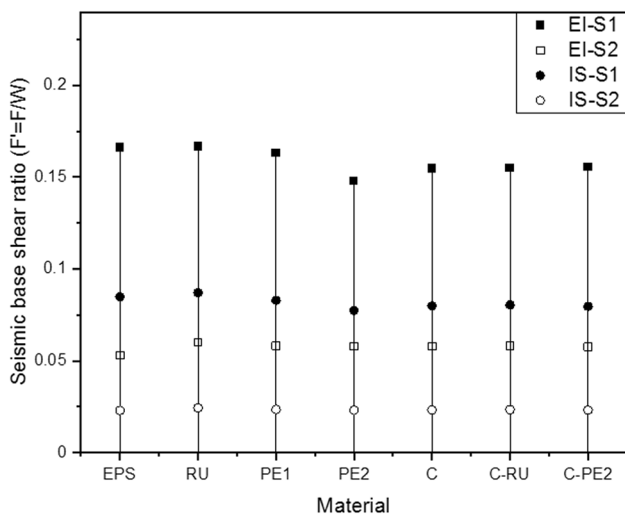


Fig. 7 Seismic base shear ratio of building on reinforced soil with various mats

Table 6 Base shear ratio for buildings on a fixed base and flexible base conditions

Earthquake	Base shear ratio (\bar{F})		
	Fixed base	Flexible base without isolation	
		Soft soil	Stiff soil
E l Centro	0.046	0.18	0.06
IS	0.015	0.10	0.03

base. The impact of SSI decreases with increasing soil stratum stiffness. Ignoring SSI for short structures supported by shallow foundations may actually underestimate the seismic response, which may be increased due to the period elongation and corresponding increase in spectral response of the fundamental mode, as demonstrated by a recent study by Dutta et al. [49] and Raychowdhury [50].

It is seen that the soil condition has a pronounced effect on building base shear response. From the analysis of soil reinforced with mats of case 2 materials, a maximum of 23 and 20% reduction in the base shear value is observed with PE₂ mat and C-PE₂ mat reinforcement in soft soil. Stiff soil condition produces less base shear in buildings. Only below 10% reduction in base shear is observed while reinforcing stiff soil with all the isolation mats under El Centro input motions (Fig. 7). Since the base shear directly depends on the input earthquake amplitude, the base shear observed in the soil–structure system subjected to El Centro motions is seen to be higher than that observed with IS input motions.

Total and differential Settlement of raft foundation

The settlement of the raft foundation should be as uniform as possible, and it should be within permissible limits too. Therefore, it is essential to avoid differential settlement rather than to maintain a uniform overall settlement of the structure. The settlement at the soil–raft foundation interface is noted, and settlements are observed to differ over the length of the raft. In the middle, the vertical settlement is very small and increased to the edge of the raft foundation. Since the soil–structure system was laterally subjected to earthquake excitations, raft sliding is highly probable. The settlement is found to be dependent on soil flexibility. That is, the settlement of the raft foundation increases with the increase in soil flexibility and the result matches with the previous results [51–53]. It is seen that soil deformation is significantly less in stiff soil since the raft foundation behaves as rigid while interacting with stiff soil.

The total permissible settlement and differential settlement for raft foundation in the sand are 0.075 m and 0.0021L' for RCC structures according to IS 1904-1978, where L'-center to center distance between columns in meters. It is found from the static analysis of the soft soil–structure system that the settlement (82 mm) (Fig. 8b) exceeds the permissible value specified in the code, and the soil must, therefore, be reinforced with a particular variety of isolation materials to enable the structures to be adequately supported from earthquake loads. The raft–soil interface is an important area where energy is transferred from earthquake motions in the soil stratum to the superstructure. This makes the settlement at the interface a very critical parameter to be evaluated before and after the soil improvements. Figure 8c, d shows the contour plot of the total settlement observed in unreinforced and C-PE₂ mat reinforced soil cases while it is excited under EL Centro input motion. At two points with a distance of L', the settlement observed on the edge of the raft foundation at a particular time when it gives the maximum value of settlement during the whole earthquake motion is noted, and their difference is considered as the differential settlement of the raft foundation.

Among the case 1 materials, the PE₂ mat reinforced soil system shows 62.7% isolation efficiency to reduce the differential settlement in soft soil under El Centro input motion (Table 7). It marks the highest reduction in the differential settlement. PE₂ mat performs about two times better over PE₁ mat for the same. The isolation efficiency of reinforcement mats in reducing the settlement at the raft–soil interface is represented in terms of reduction factor (RFs) in Fig. 9 (where 'L'-length of the raft foundation). The deflection of the raft foundation is not significantly reduced by reinforcing with EPS mat in soft soil. High-stiff reinforcement materials reduce the seismic response of the building in soil [7]. Under IS input motion, a maximum reduction

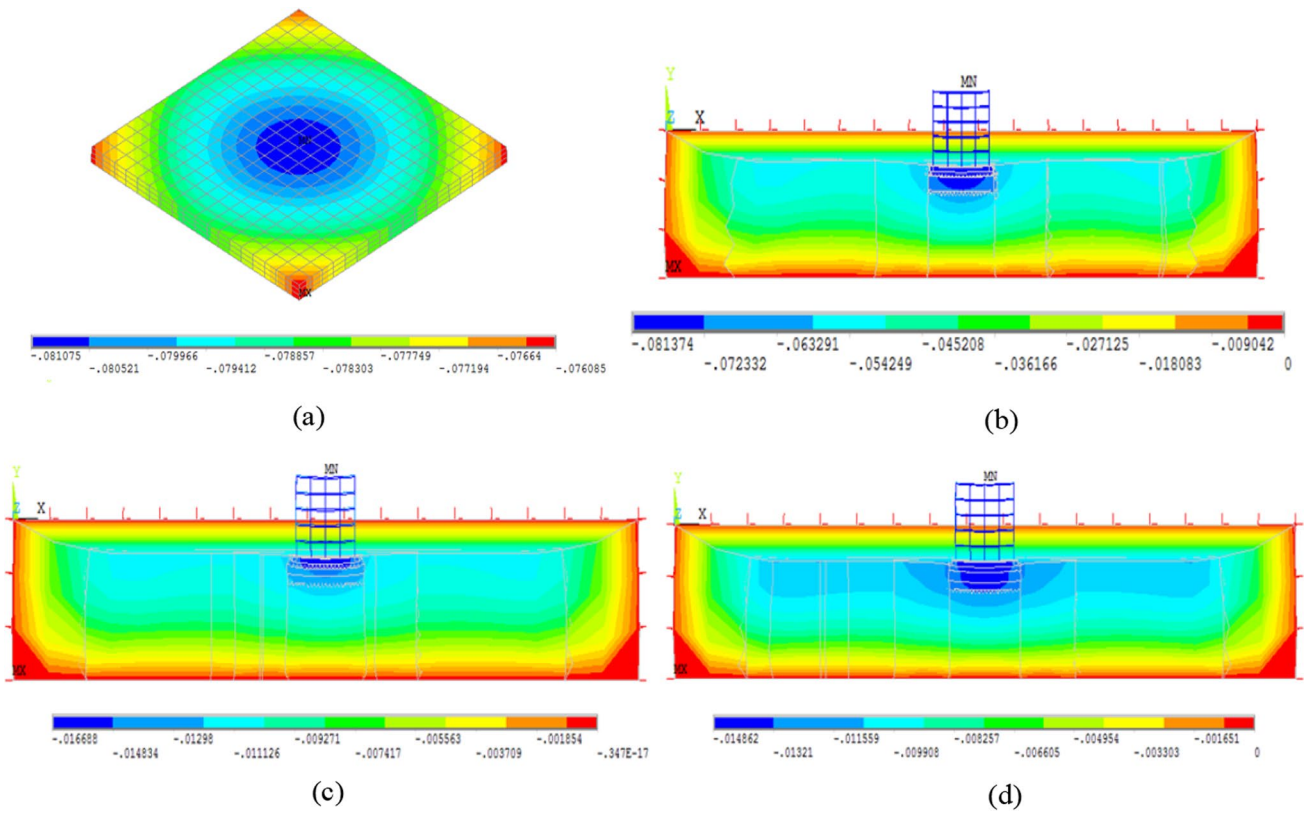


Fig. 8 Settlement of raft foundation resting on soft soil under static loading **a** along the length of raft foundation on the unreinforced soil **b** cross section of the unreinforced soil–structure system **c** rubber

reinforced soil–structure system **d** coir reinforced soil–structure system; Settlement in soft soil under El Centro motions

Table 7 Percentage reduction in differential settlement of raft foundation

Soil type	Input motion	Percentage reduction in differential settlement of raft foundation (%)						
		EPS	RU	PE ₁	PE ₂	C	C-RU	C-PE ₂
Soft	El Centro	12	27.2	35.8	62.7	46.6	44.1	50.1
	IS	5	25.2	32.6	58.5	40.7	39	39.9
Stiff	El Centro	10	16	30	43.2	42.1	41.1	42.5
	IS	4.5	11	20	37.4	37	36.6	30

factor of 1.49 and 2.37 is obtained for the soft soil reinforced with PE₁ and PE₂ mats (Fig. 9c). In stiff soil, neither EPS nor RU mat reinforcement could reduce the settlement significantly when the SSI system is subjected to both the input motions.

From the study of soil strengthened with mats of case 2 materials, the C-PE₂ mat reinforced soft and stiff soil considerably reduces the differential settlement at the raft edges by about 50.1 and 42.5%, respectively, from unreinforced soil when it is excited under El Centro motions. The settlement is seen to be higher on the edges of the raft since the input motion has been applied to the soil structural system laterally. From the analysis carried out to study the efficacy of isolation mats to reduce the differential settlement of raft

foundation, it is concluded that differential settlement values seen for various isolated SSI systems analyzed under two different earthquake excitations were within permissible limits as per the code. The reinforcing mats give good RFs values for the soil–structure system excited under El Centro input motions compared to IS input motions. PE₂ and C-PE₂ mats are found to be more effective in reducing differential settlement of the raft foundation.

Contact pressure distribution at raft–soil interface

In the SSI system with different mat reinforced cases, the contact pressure distribution below the raft foundation is analyzed by considering soil flexibility. From the response of

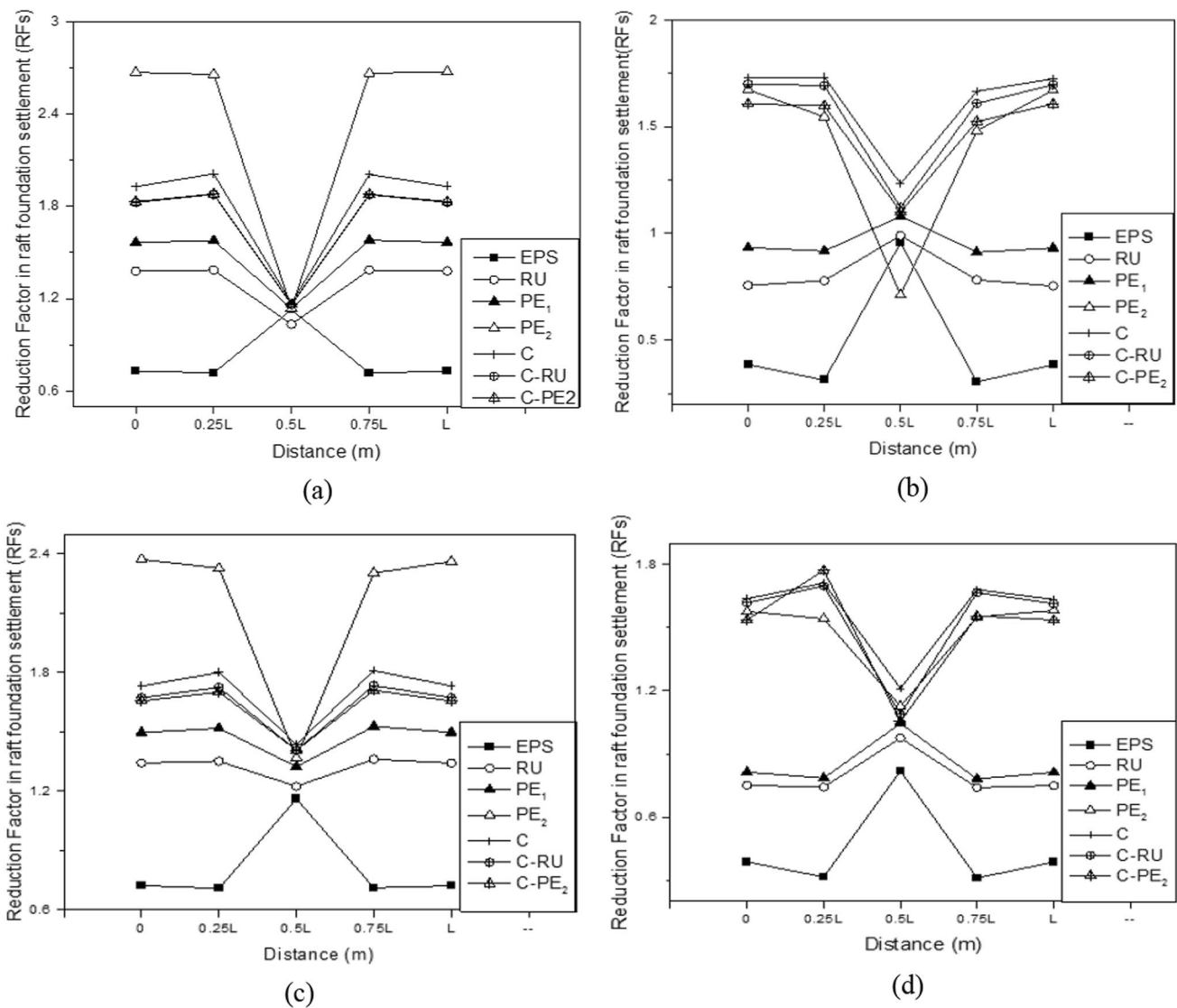


Fig. 9 Reduction factor for vertical settlement along the length of the raft foundation under **a** El Centro-soft soil **b** El Centro-stiff soil **c** IS-soft soil **d** IS-stiff soil

the soil foundation interface on the application of dynamic load, it is noticed that the contact pressure distribution on the edge of the soil foundation is higher and decreasing toward the center.

Soil reinforcement reduces the contact pressure development under earthquake loads at the raft–soil interface. The decrease in contact pressure in terms of the reduction factor is shown in Fig. 7 for reinforced soil from that of unreinforced soil system, where 'L'-length of the raft foundation. Among case 1 materials, PE₁ and PE₂ mat reinforcement in soft soil subjected to El Centro input motion show 37.7 and 49% isolation efficiency in reducing the contact pressure. PE₂ mat reinforcement in soft soil significantly reduced the contact pressure across the raft base with a maximum reduction factor of 1.96 (Fig. 10a). Rubber mat could act

as good isolation material by reducing pressure distribution with a reduction factor of 1.3, i.e., about 22% reduction compared to unreinforced soft soil. EPS geofoam material is not efficient in reducing the differential settlement, but this reinforcement in soft soil reduces the contact pressure at the raft–soil interface. With EPS mat reinforcement in soft soil, around a 15% reduction in contact pressure from unreinforced soil is observed.

The pressure development under dynamic loads is influenced by soil flexibility. Stiff soil has high density and modulus of elasticity values. The findings show that the intensity of contact pressure is increased with an increase in the stiffness of the soil. Contact pressure developed beneath the raft base is 51.67% in the stiff soil than that of soft soil in the unreinforced soil–structure system. A contact pressure

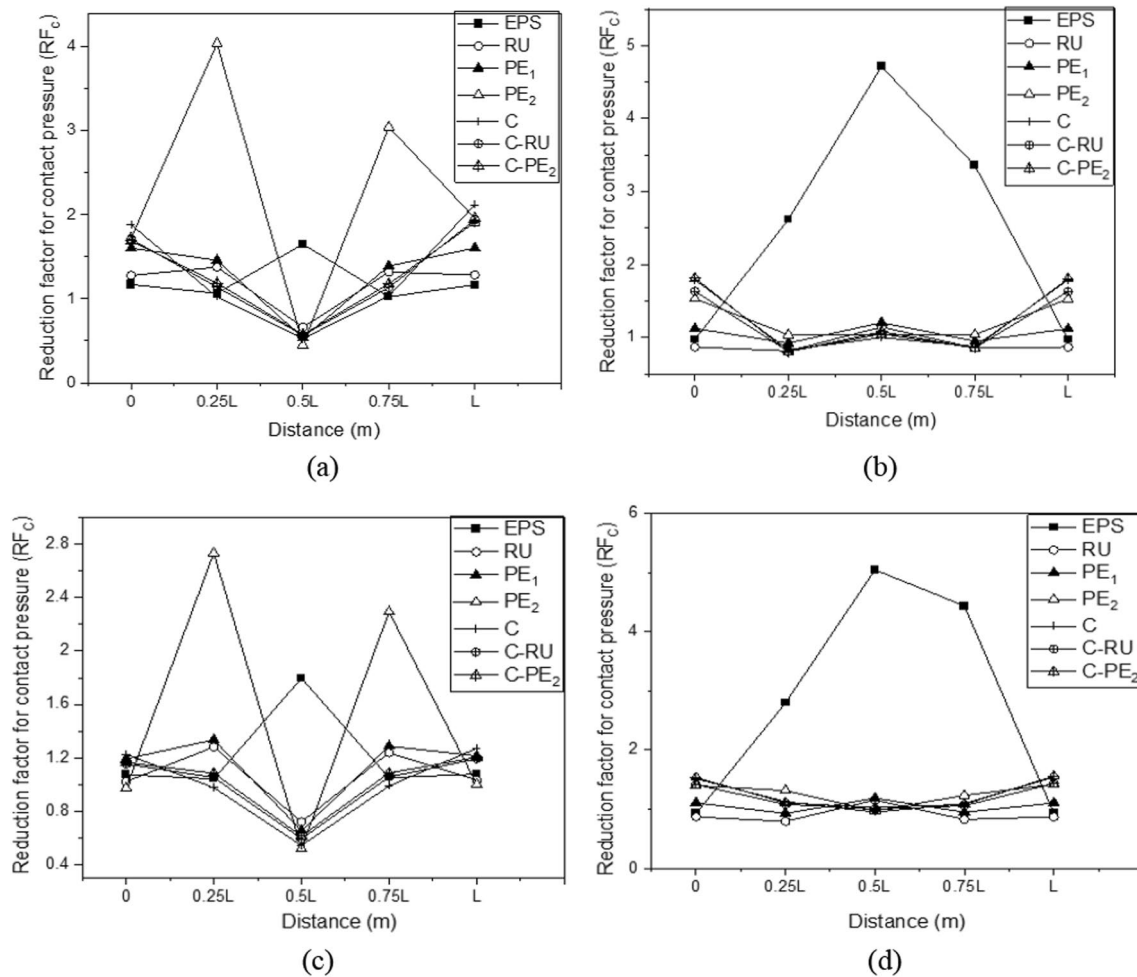


Fig. 10 Reduction factor for contact pressure distribution along the length of the raft foundation under **a** El Centro-soft soil **b** El Centro-stiff soil **c** IS-soft soil **d** IS-stiff soil

reduction factor (RF_c) of 1.12 and 1.53 is seen in stiff soils, respectively, with PE₁ and PE₂ mat reinforcement. A noticeable reduction in the pressure development below the raft foundation is not observed with the stiff soil enhanced by the RU mat.

Contact pressure developed below the raft foundation under IS input motion is examined. Under El Centro input motions, reinforced mats show higher isolation efficiency than under IS input motions. The maximum reduction in contact pressure is with PE₂ mat reinforcement in soft soil with an RF_c of 1.2 and stiff soil with an RF_c of 1.4 (Fig. 10c, d).

For soft soil reinforced with the mats of case 2 materials, excited under El Centro input motion, coir mat strengthened soft soil show a maximum RF_c value among case 2 materials, which is about 2.1 (Fig. 10a). A reduction factor of about 1.9 is observed from C-RU, and C-PE₂ mats enhanced soft soil. All the isolation mats impart their influence in efficiently reducing the seismic responses. The coir mat

reinforcement reduced the contact pressure nearly equally in soft and stiff soils by about 44–53%.

For the soil–structure system subjected to IS input motions, a maximum of 22 and 36% pressure reduction is observed below the raft foundation with coir mat reinforcement in soft and stiff soil, respectively. The current study inferred from the analysis of contact pressure induced at the raft–soil interface that the SSI effect is negligible for buildings built on stiff soil, but it increases with increased soil flexibility. Earlier studies also show the same results that with the increase in stiffness of soil contact pressure increase [54–58].

Conclusion

The current numerical analysis investigates the seismic isolation effect of the reinforcement mats placed in the soil below the raft foundation as an isolation medium. The efficacy of

the isolation mats to mitigate the seismic response of the raft foundation and the superstructure is evaluated with parametric studies by transient analysis of three-dimensional finite element models of the soil–structure system in ANSYS. From the research carried out on the SSI system with and without reinforcement, the following conclusions are drawn:

- The seismic response of buildings is expressed in terms of maximum response of roof acceleration and base shear, and that of raft foundation is represented in terms of maximum response of total and differential settlement and contact pressure.
- As soil flexibility increases, seismic responses increase. The natural frequency of the SSI system is lower than the natural frequency of the fixed-base structure (1.96 Hz), and about 43% reduction in natural frequency was noticed when the underlying soil was soft. The roof acceleration of the building is increased by about 70 and 33%, respectively, in soft and stiff soil base supported system, compared to the fixed-base system subjected to El Centro input motion (Fig. 4).
- The reinforcement of soft soil by the isolation mats effectively reduces seismic responses of building and raft foundation compared with the reinforcement done with stiff soil. And these materials are found to be performing well under input earthquake motion of higher amplitude.
- A maximum reduction in the building roof acceleration and base shear is observed about 23 and 23% by reinforcing soft soil with C-PE₂ and PE₂ mats. Base shear is higher for buildings resting on a flexible base compared to fixed-base conditions.
- The PE₂ and C-PE₂ mats used as soil reinforcement materials effectively reduce the differential settlement of raft foundation compared to the other isolation materials. The PE₂ and C-PE₂ mats used result in an isolation efficiency of 62.7 and 50.1%, respectively. The maximum reduction factor (RFs) of 2.4–2.7 was observed for PE₂ mat reinforcement in soft soil and about 1.8 for coir mat and its composites in stiff soil. This reduces the total raft settlement.
- The maximum reduction in contact pressure induced at the raft–soil interface is found to be about 49 and 53% when the soft soil is reinforced with PE₂ mat and coir mat materials respectively.
- It is inferred from this proposed study, the performance analysis of the isolation mats; coir mat with its composites, and high stiff polyethylene (PE₂) mat act as good isolation mats under both the input motions with PGA 0.1 g and 0.3 g. The use of the coir products as isolation medium in the soil will be economically beneficial as it is a natural way of isolating the soil domain than standard isolation methods. The coir mat composited with PE₂ mat improves the durability of the coir mat by protecting it

from biodegradation and also act as a suitable drainage medium. Therefore, from the analysis, it is suggested to reinforce the soil with the C-PE₂ composite mat as a seismic isolation medium.

Author contributions All authors contributed to the study conception and design. Material preparation, data collection, and analysis were performed by Sreya MV. The first draft of the manuscript was written by Sreya MV and all authors commented on previous versions of the manuscript. All authors read and approved the final manuscript.

Funding No funding was received for conducting this research.

Data availability The datasets generated during and/or analyzed during the current research are available from the corresponding author upon reasonable request.

Declarations

Conflict of interest On behalf of all authors, the corresponding author states that there is no conflict of interest.

Ethical approval This article does not contain any study with human participants or animals performed by any of the authors.

Informed consent For this type of study formal consent is not required.

References

1. Tsang HH (2008) Seismic isolation by rubber-soil mixtures for developing countries. *Earthquake Eng Struct Dyn* 37(2):283–303.
2. Ahmed I (1993) Laboratory study of properties of rubber-soils. Final Rep., Indiana Dept. of Transp., Joint Highway Research Project, Purdue Univ., West Lafayette, IN.
3. Aaboe R (1987) 13 years of experience with expanded polystyrene as lightweight fill material in road embankments, vol 61. Norwegian Road Research Laboratory Publication, Norway, pp 21–27
4. Sheeley M (2000) Slope stabilization utilizing geofoam. Master's Thesis, Syracuse University, New York.
5. AbdelSalam SS, Azzam S, Fakhry BM (2017) Reliability and 3D modeling of flexible walls with EPS inclusion. *Int J Geomech* 17(7):04016153
6. Khan MI, Meguid MA (2018) Experimental investigation of the shear behavior of EPS geofoam. *Int J Geosyn Ground Eng* 4(2):1–12
7. Riad HL, Ricci AL, Osborn PW, Horvath JS (2003) Expanded polystyrene (EPS) geofoam for road embankments and other lightweight fills in urban environments. In: Soil and rock America, 12th Pan-American conference on soil mechanics and geotechnical engineering and 39th US rock mechanics symposium, vol 6
8. Stark TD, Arellano D, Horvath JS, Leshchinsky D (2004) “Geofoam applications in the design and construction of the international conference on geotechnical engineering for coastal development,” pp 783–788 Theses u-shaped geofoam wrap. *Int J Geosynth Ground Eng* 3(2):11
9. Zarnani S, Bathurst RJ (2007) Experimental investigation of EPS geofoam seismic buffers using shaking table tests. *Geosynth Int* 14(3):165–177
10. Bartlett S, Arellano D, Vaslestad J, Aabøe R, Ahmed T (2018) Bridge foundations supported by EPS geofoam embankments on

- soft soil. In: Proceedings of the 5th international conference on geofam blocks in construction applications, Kyrenia, Cyprus, pp 9–11.
11. Meguid M, Hussein M, Ahmed M, Omeman Z, Whalen J (2017) Investigation of soil–geosynthetic–structure interaction associated with induced trench installation. *Geotextiles Geomembrane* 45(4):320–330.
 12. Vaslestad J, Bartlett SF, Aabøe R, Burkart H, Ahmed T, Arellano D (2019) Bridge foundations supported by EPS geofam embankments on soft soil. In: 5th international conference on geofam blocks in construction applications (pp. 281–294). Springer, Cham.
 13. El-kady MS, Alzara MA, Farouk MA (2018) Reduction of lateral earth pressure using Geo-fam blocks. *Innov Infrastruct Solut* 3(1):1–5
 14. Jutkofsky WS, Teh Sung J, Negussey D (2000) Stabilization of embankment slope with geofam. *Transp Res Rec* 1736(1):94–102
 15. Negussey D (2002) Slope stabilization with geofam. Report to FHWA and the EPS industry. Geofam Research.
 16. Ramli Sulong NH, Mustapa SAS, Abdul Rashid MK (2019) Application of expanded polystyrene (EPS) in buildings and constructions: a review. *J Appl Polym Sci* 136(20):47529
 17. Sridhar RS, Prabakar (2002) Effect of random inclusion of sisal fiber on the strength behavior of soil. *Construct Build Mater* 16(2):123–131.
 18. Abu-Hejleh N, Zornberg J G, Elias V, Watcharamonthein J (2003) Design assessment of the founders/meadows GRS abutment structure. In: Proceeding on 82nd annual TRB meeting.
 19. Orman E (1994) Interface shear strength properties of roughened HDPE. *J Geotech Eng ASCE* 120:758–761
 20. Consoli NC et al. (2002) Engineering behavior of a sand reinforced with plastic waste. *J Geotechn Geoenviron Eng* 128(6):462–472. [https://doi.org/10.1061/\(ASCE\)1090-0241\(2002\)128:6\(462\)](https://doi.org/10.1061/(ASCE)1090-0241(2002)128:6(462)).
 21. Park T, Tan SA (2005) Enhanced performance of reinforced soil walls by the inclusion of short fiber. *Geotextiles Geomembranes* 23 (4):348–361. <https://doi.org/10.1016/j.geotexmem.2004.12.002>.
 22. Patil SJ, Reddy GR (2012) State of the art review-base isolation systems for structures. *Int J Emerg Technol Adv Eng* 2(7):438–453
 23. Srilatha N, Latha GM, Puttappa CG (2016) Seismic response of soil slopes in shaking table tests: effect of type and quantity of reinforcement. *Int J Geosyn Ground Eng* 2(4):1–13
 24. Yegian MK, Lahlaf AM (1992) Geomembranes as base isolation. Geosynthetic fabric report *J Geotech Eng* 4(18):643–645
 25. Nanda RP, Dutta S, Das A, Khan HA (2017) Geosynthetic liner as foundation isolation for seismic protection. *Int J Geosyn Ground Eng* 3(3):21
 26. Boominathan A, Hari S (2002) Liquefaction strength of fly ash reinforced with randomly distributed fibers. *Soil Dyn Earthquake Eng* 22(9):1027–1033.
 27. Keramatikerman M, Chegenizadeh A, Nikraz H (2017) Experimental study on the effect of fly ash on liquefaction resistance of the sand. *Soil Dyn Earthq Eng* 93:1–6
 28. Maheshwari BK, Singh HP, Saran S (2012) Effects of reinforcement on liquefaction resistance of Solani sand. *J Geotechn Geoenviron Eng* 138 (7):831–840.
 29. Haque MM, Ali ME, Hasan M, Isla MN, Kim H (2012) Chemical treatment of coir fiber reinforced polypropylene composites. *Ind Eng Chem Res* 51(10):3958–3965
 30. Kumar A, Gupta D (2016) Behavior of cement-stabilized fiber-reinforced pond ash, rice husk ash–soil mixtures. *Geotext Geomembr* 44(3):466–474
 31. Munirah Abdullah N, Ahmad I (2012) Effect of chemical treatment on mechanical and water-sorption properties coconut fiber-unsaturated polyester from recycled PET. *ISRN Materials Science*.
 32. Sultana Mir S, Hasan M, Hasan SM, Hossain MJ, Nafsin N (2017) Effect of chemical treatment on the properties of coir fiber reinforced polypropylene and polyethylene composites. *Polym Compos* 38(7):1259–1265
 33. Wolf JP (1985) Dynamic soil-structure interaction. Prentice-Hall, New York
 34. Makris N, Chang S-P (2000) Effect of viscous, viscoplastic and friction damping on the response of seismic isolated structures. *Earthquake Eng Struct Dyn* 29(1):85–107.
 35. Majumder M, Ghosh P (2015) Finite element analysis of vibration screening techniques using EPS geofam. In: Computer methods and recent advances in geomechanics: proceedings of the 14th international conference of international association for computer methods and recent advances in geomechanics, 2014 (IACMAG 2014) (pp. 649–654). Taylor & Francis Books Ltd, New York.
 36. Santoni L, Webster L (2001) Airfields and road construction using fiber stabilization of sands. *J Trans Eng ASCE* 127:96–104.
 37. Gu Q, Liu Y, Li Y, Lin C (2018) Finite element response sensitivity analysis of three-dimensional soil-foundation-structure interaction (SFSI) systems. *Earthq Eng Eng Vib* 17(3):555–566
 38. Liu J, Tan H, Bao X, Wang D, Li S (2019) Seismic wave input method for three-dimensional soil-structure dynamic interaction analysis based on the substructure of artificial boundaries. *Earthq Eng Eng Vib* 18(4):747–758
 39. Tsai CS, Hsueh CI, Su H (2016) Roles of soil-structure interaction and damping in base-isolated structures built on numerous soil layers overlying a half-space. *Earthq Eng Eng Vib* 15(2):387–400
 40. Babu KK, Beena KS (2007) Utilisation of coir geotextiles for unpaved roads and embankments. Doctoral dissertation, Cochin University of Science and Technology
 41. Duskov M (1991) Use of expanded polystyrene (EPS) in flexible pavements on poor subgrades. In: Proceedings of the international conference on geotechnical engineering for coastal development, pp 783–788
 42. Krishnaswami NR, Isaak NT (1995) Liquefaction analysis of saturated reinforced granular soils. *J Geotech Eng* 121(9):645–651
 43. Rajeswari JS, Sarkar R, Roy N, Bharti SD (2019) Bearing capacity of circular footing supported on coir fiber-reinforced soil. *Int J Geotechn Eng* 13(3):218–226.
 44. ASTM International, ASTM D7180 (2013) "Standard Guide for the use of Expanded Polystyrene (EPS) Geofam in Geotechnical Projects."
 45. ASTM International, ASTM D5321 (2017) "Standard Test Method for Determining the Coefficient of Friction by the Direct Shear Method"
 46. Jayalekshmi BR, Chinmayi HK (2016) Effect of soil stiffness on seismic response of reinforced concrete buildings with shear walls. *Innov Infrastruct Solut* 1(1):2
 47. Sharma N, Dasgupta K, Dey A (2018) A state-of-the-art review on seismic SSI studies on building structures. *Innov Infrastruct Solut* 3(1):1–16
 48. Soneji BB, Jangid RS (2008) Influence of soil–structure interaction on the response of seismically isolated cable-stayed bridge. *Soil Dyn Earthq Eng* 28(4):245–257
 49. Dutta SC, Bhattacharya K, Roy R (2004) Response of low-rise buildings under seismic ground excitation incorporating soil–structure interaction. *Soil Dyn Earthq Eng* 24(12):893–914
 50. Raychowdhury P (2009) Effect of soil parameter uncertainty on seismic demand of low-rise steel buildings on dense silty sand. *Soil Dyn Earthq Eng* 29(10):1367–1378
 51. Jayalekshmi BR, Jisha SV, Shivashankar R (2017) Analysis of foundation of tall R/C chimney incorporating flexibility of soil. *J Inst Eng (India) Series A* 98(3):211–217.

52. Korff M, Mair RJ, Van Tol FA (2016) Pile-soil interaction and settlement effects induced by deep excavations. *J GeotechGeoenviron Eng* 142(8):04016034
53. Qiang LUO, Qing-yuan LU (2018) Settlement calculation of rigid pile composite foundation considering pile-soil relative slip under embankment load. *China J Highway Transport* 31(1):20
54. Bhattacharjee T, Chanda D, Saha R (2021) Influence of soil flexibility and plan asymmetry on seismic behaviour of soil-piled raft-structure system. In: *Structures* (Vol. 33, pp. 1775–1788). Elsevier, Amsterdam
55. Edil TB, Bosscher PJ (1994) Engineering properties of tire chips and soil mixtures. *Geotech Testing J* 17(4):453–464
56. Jisha SV, Jayalekshmi BR, Shivashankar R (2012) Contact pressure distribution under raft foundation of tall reinforced concrete industrial chimneys due to dynamic soil-structure interaction. ISET golden jubilee symposium Indian Society of Earthquake Technology.
57. Lu Y, Hajirasouliha I, Marshall AM (2016) Performance-based seismic design of flexible-base multi-storey buildings considering soil–structure interaction. *Eng Struct* 108:90–103
58. Tabatabaiefar HR, Clifton T (2016) Significance of considering soil-structure interaction effects on seismic design of unbraced building frames resting on soft soils. *Aust Geomech J*

Springer Nature or its licensor (e.g. a society or other partner) holds exclusive rights to this article under a publishing agreement with the author(s) or other rightsholder(s); author self-archiving of the accepted manuscript version of this article is solely governed by the terms of such publishing agreement and applicable law.